Nucleic Acids Research, 1996, Vol. 24, No. 15 **3065–3070**

RNase E processing of essential cell division genes mRNA in *Escherichia coli*

Kaymeuang Cam*, Gilles Rome, Henry M. Krisch and Jean-Pierre Bouché

Laboratoire de Microbiologie et Génétique Moléculaire, Centre National de la Recherche Scientifique, 118 route de Narbonne, 31062 Toulouse, France

Received February 16, 1996; Revised and Accepted June 20, 1996

ABSTRACT

The ratio of the FtsZ to FtsA proteins determines the correct initiation of cell division in *Escherichia coli*. The genes for these proteins are contiguous on the chromosome. Although both genes are transcribed from common promoters, the presence of *ftsZ*-specific promoters, along with differences in the efficiency of translation of their respective mRNAs, contribute to the increased relative expression of *ftsZ*. We report here that the polycistronic *ftsA–ftsZ* transcripts are cleaved by RNase E and that this cleavage affects the decay of *ftsA* and *ftsZ* mRNA. As a consequence of the cleavage, RNase E also contributes to the differential expression of the two genes.

INTRODUCTION

Cell division in *Escherichia coli* requires the products of several essential genes. The data obtained from many laboratories point to *ftsZ* as a gene playing a central role in this process (1). *ftsZ* is the target of all the known endogenous cell division inhibitors (2), and changing its level of expression affects the position of the septa, the frequency and the timing of division (3–5). Gene *ftsZ* is located at 2 min on the genome, in a cluster that includes genes involved in both cell division and in peptidoglycan synthesis. Expression of *ftsZ* is inversely correlated with growth rate so that the quantity of the protein is nearly constant (6). This result lead to the notion that a fixed number of FtsZ molecules is required for cell division. However, this idea has been challenged (7).

Immediately upstream from *ftsZ* lie two other cell division genes, *ftsQ* and *ftsA* (Fig. 1). The abundance of the three gene products in the cell is ~25 molecules of FtsQ (8), 200 of FtsA (9) and 5000–20 000 of FtsZ (10,11). Six promoters were reported (6), which account for 50–80% of *ftsZ* mRNA (12,13). No transcription terminator has been identified in the region. Mukherjee and Donachie reported that *ftsZ* is translated more efficiently than *ftsA* which in turn is translated more efficiently than *ftsQ* (14). The difference in the level of transcription of each gene and in the efficiency of translation of the mRNAs could explain the substantial differences observed in the expression of the three genes. At least for FtsA and FtsZ, the molar ratio is important for cell division to occur correctly, since filamentation induced by overexpression of one gene is suppressed by increased expression of the other (15,16).

This work reports the characterization of RNase E cleavage sites affecting the decay of *ftsA* and *ftsZ* mRNAs. We propose that RNase E contributes to the differential expression of *ftsZ* versus *ftsA* (and also possibly *ftsQ*).

MATERIALS AND METHODS

Bacterial strains and plasmids

Experiments were carried out with isogenic strains N3431 (*rne3071*^{ts}) and N3433 (*rne*$^{+}$) (17) transformed with pZAQ (3), a pBR322 plasmid derivative in which *ftsQ–ftsA–ftsZ* region was cloned (Fig. 1). Without this high copy plasmid, transcription of the chromosomal copy of the operon was too low to obtain a primer extension signal.

pKC107 is the pGEM2 plasmid (from Promega Corp.) on which the *Pst*I–*Cla*I fragment from pZAQ containing *ftsQ–ftsA–ftsZ* genes has been cloned between the *Pst*I and *Sma*I sites. In this construction, all three genes can be jointly transcribed from the vector T7 promoter.

RNA preparation and analysis

Cells were grown at 32°C in Luria broth supplemented with tetracycline (15 µg/ml), and shifted to 43°C for 10 min to inactivate RNase E. Then, as required, rifampicin was added at 150 µg/ml. RNA was extracted as described by Sarmientos *et al.* (18). In the experiments shown in Figures 5 and 6, samples were further treated with DNase I, although we found that this treatment does not alter the results. Primer extension and quantitative S1 protection experiments were performed as described by Cam *et al.* (19) and Theisen *et al.* (20) respectively. The oligonucleotides used to identify RNase E cleavage sites were 5′-GCGAAGAATTCAACACCTTCAATGC (PE1) and 5′-GAGTCGCTTGATCCACGAGCC (PE2). They are complementary to the beginning of *ftsZ* and the end of *ftsA* respectively. The two oligomers used in the S1 protection experiments were complementary to the coding region near the 5′ end of either *ftsA* or *ftsZ*, except for the 9 and 8 nt at the 3′ end respectively. *ftsA* and *ftsZ* oligomers were 60 and 43 nt long respectively and their sequences are: 5′-TCCCCTACTAAAGCGGCAACCTTCGCGGTACCAATCTCCAGTCCTACTACCTCAAAAGAC (SE2)and 5′-ATTTGAATCGTCTGTCCAACCGCTGTTTTACGCAGACAAACAC (SE1).

* To whom correspondence should be addressed

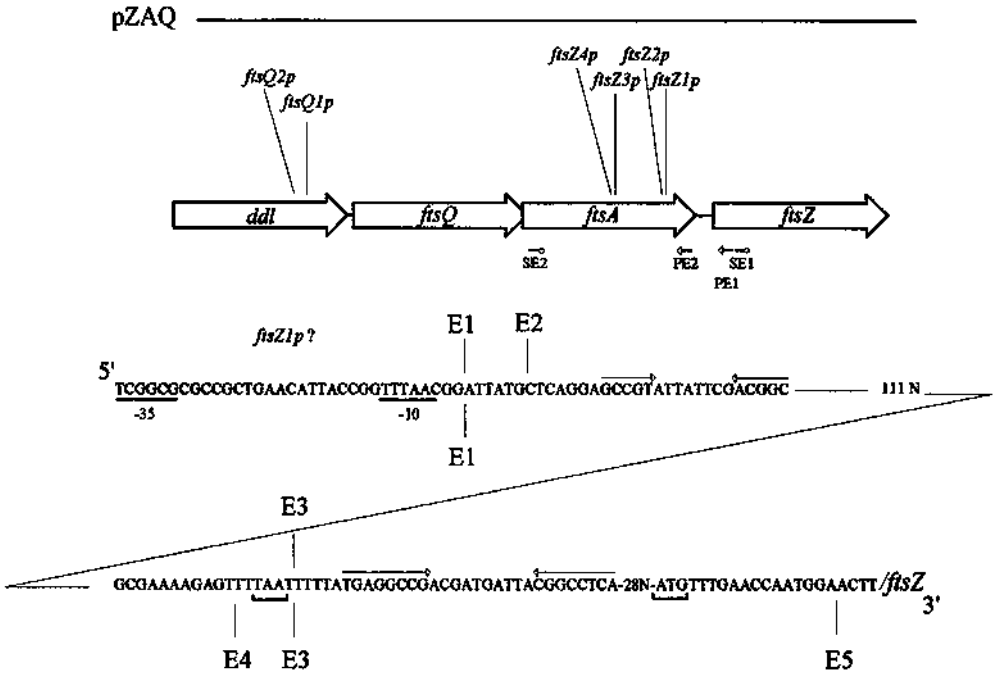

Figure 1. Location of RNase E cleavage sites. The top of the figure presents the genetic organization in the *ddl–ftsZ* region. The fragment cloned in the pZAQ plasmid is shown. The two *ftsQ* and the four *ftsZ* promoters tentatively identified by S1 protection experiments in *ddl* and *ftsA* genes respectively are indicated (6), as well as the probes (PE1, PE2, SE1 and SE2) described in Materials and Methods. The bottom of the figure presents the sequence around the RNase E cleavage sites. –35 and –10 boxes are those proposed for *ftsZ1p* promoter sequence (6). Underlined are *ftsA* gene TAA stop codon and *ftsZ* gene ATG start codon. Inverted arrows indicate potential stem–loop structures. E1, E2, E3 shown above the sequence are the cleavage sites identified *in vivo* in the experiment of Figure 2, while E1, E3, E4, E5 shown below are those identified *in vitro*.

Both oligomers were mixed with a molar ratio of 1:1, then labeled at their 5′ end, hybridized overnight at 40°C with cellular RNA and digested with S1 nuclease for 90 min at 30°C. Signals in the gels were quantitated with a Phosphor-Imager.

In order to normalize the results of the S1 protection experiment, in the experiment shown in Figure 4, the mixture of oligomers was also used to protect RNA synthesized *in vitro* with T7 RNA polymerase, using as template pKC107 plasmid linearized by *Bst*EII enzyme, which makes a unique cleavage at the 3′ end of *ftsZ* coding sequence.

In vitro cleavage by RNase E

Reactions with purified RNase E enzyme were performed according to Carpousis *et al.* (21). Inactivation of mutant RNase E was achieved by heating the enzyme at 43°C for 10 min. Purified RNA (1 µg) synthesized *in vitro* from pKC107 as described above was used as substrate in a 10 µl reaction. One tenth of this reaction was analyzed by primer extension.

RESULTS

ftsZ1p mRNA is an RNase E-dependent cleavage product

By S1 mapping analysis (6), six major 5′ ends had been previously identified in the 3 kb region upstream *ftsZ* (Fig. 1). Two are located upstream of *ftsQ*, in the *ddl* coding sequence (*ftsQ1p*, *ftsQ2p*) while four are in the *ftsA* coding sequence (*ftsZ1p*, *ftsZ2p*, *ftsZ3p*, *ftsZ4p*). However none of these 5′ ends were located at an appropriate distance from a sequence with strong homology to the canonical σ^{70} promoter sequence, raising

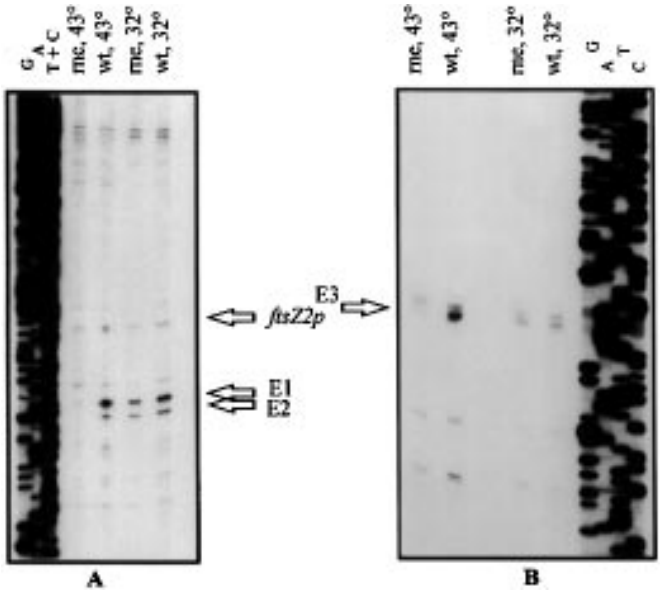

Figure 2. Identification of RNase E cleavage sites *in vivo*. Primer extension analysis was performed on RNA from wild-type and *rne* strains grown at 32°C and shifted at 43°C for 10 min. (**A**) Extension reactions using PE2. (**B**) Extension reactions using PE1. E1, E2 (A) and E3 (B) indicate the RNase E cleavage sites. The 5′ end generated by the *ftsZ2p* promoter is also shown. The same oligonucleotides were used to make the pZAQ sequence ladders shown (G, A, C, T, C+T).

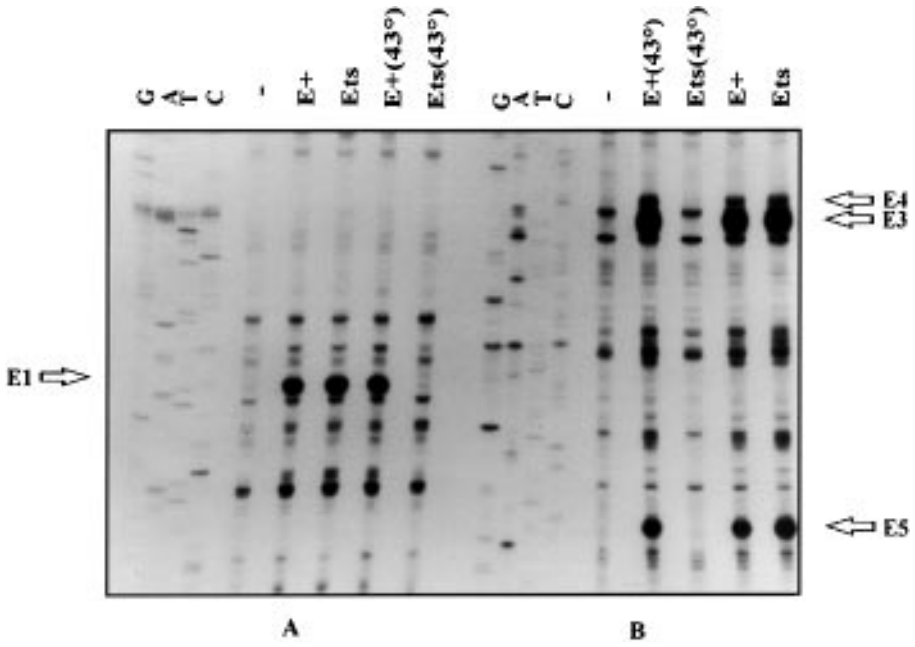

Figure 3. Identification of RNase E cleavage sites *in vitro*. Purified wild-type (E+) or thermolabile mutant (Ets) RNase E enzymes were used. The enzymes were added directly to the reactions (lanes E+ and Ets), or previously heated at 43°C for 10 min [lanes E+(43°) and Ets(43°)]. In one instance no enzyme was added (lane –). Reactions were done at 30°C. Primer extension analysis was performed on RNase E digestion products generated *in vitro*. (**A**) Extension reactions using PE2. (**B**) Extension reactions using PE1. E1 (A) and E3, E4, E5 (B) indicate the RNase E cleavage sites. The same oligonucleotides were used to generate the pZAQ sequence ladders shown (G, A, T, C).

the possibility that some of the RNA species detected by the S1 protection experiment might be products of endonucleolytic cleavages. Examination of the sequence suggested a potential RNase E cleavage site at the RNA 5′ end attributed to promoter *ftsZ1p* (Fig. 1). Such cleavage sites occur within an A–U-rich sequence that is frequently followed by a stem–loop structure (22–24).

To determine whether *ftsZ1p* mRNA is a product of RNase E cleavage, RNA was extracted from isogenic wild-type and *rne(ts)* strains carrying *ftsQAZ*$^+$ plasmid pZAQ (see Materials and Methods), and then analyzed by primer extension with primer PE2. In the wild-type background (Fig. 2A), two closely spaced 5′ ends were detected, E1 and E2. In the *rne(ts)* background at 43°C neither of these RNA species was observed (Fig. 2A), indicating that these 5′ ends are generated by RNase E-dependent cleavages and not by transcription initiating at *ftsZ1p*. In contrast, RNA species attributed to the activities of *ftsQ1p*, *ftsQ2p*, *ftsZ4p*, *ftsZ3p*, *ftsZ2p* promoters were detected in both backgrounds (data not shown, except for *ftsZ2p*, Fig. 2A). The more efficiently cut E1 cleavage site GAUUA resembles most RNase E sites (Fig. 1) whereas weaker E2 site diverges from these sites with the cut occurring between G and C nucleotides (see below). Such a situation with a minor RNase E-dependent cleavage site next to a major site, has been reported for T4 phage transcripts (25).

ftsA–ftsZ intergenic sequence is also cleaved by RNase E

Analysis of *ftsZ* mRNA with primer PE1 complementary to the *ftsZ* coding sequence revealed another RNase E-dependent RNA species whose 5′ end, E3, is 1 nt downstream from the *ftsA* stop codon (Fig. 2B). The sequence AAU/UU where cleavage occurs conforms to the RNase E five-base A–U-rich consensus sequence (22,23). It is worth noting that a significant stem–loop structure (ΔG = –12.7 kcal) is found downstream from that sequence (Fig. 1).

In vitro cleavage by RNase E

In order to confirm that the cuts observed *in vivo* are caused by RNase E, and not by another endonucleolytic activity (26), *ftsA–ftsZ* RNA synthesized *in vitro* with T7 RNA polymerase from pKC107 template (see Materials and Methods) was incubated with purified wild-type or temperature-sensitive RNase E (21). The digestion products were analyzed by primer extension. As shown in Figure 3, the E1 and E3 sites were cleaved *in vitro* by RNase E, but not by the thermolabile enzyme that was heat-inactivated. This result confirms that *ftsZ* mRNA is processed *in vivo* by RNase E at sites E1 and E3. In contrast, the minor E2 site was not cleaved *in vitro*, suggesting that the product observed *in vivo* is not directly due to RNase E, but to another nuclease whose cleavage at this site requires RNase E activity. Two other RNase E cleavage sites were observed *in vitro* but not *in vivo*. A relatively minor one, E4, lies just upstream of the E3 site in *ftsA* coding sequence and a strong site, E5, is at the beginning of *ftsZ* coding sequence. It is conceivable that efficient *in vivo* translation of *ftsZ* inhibits cleavage at E5 (27). Alternatively, the differences in cleavage efficiency may result from the digestion conditions employed for the purified enzyme.

The ratio of *ftsA* to *ftsZ* mRNA is affected by RNase E

In primer extension experiments, accumulation of high molecular RNA species in the *rne(ts)* strain at non-permissive temperature was observed, suggesting that RNase E cleavage affects the integrity of *ftsQ–ftsA* mRNA (data not shown). To confirm this observation, the abundance of *ftsA* and *ftsZ* mRNAs was analyzed

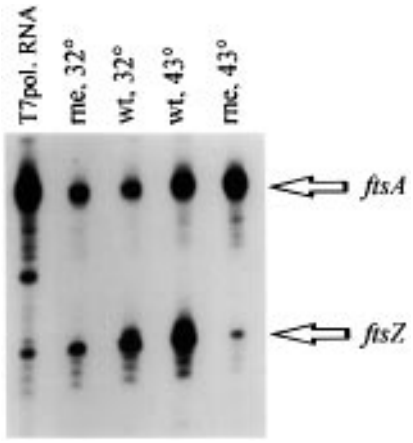

Figure 4. Quantitation of relative *ftsA/ftsZ* mRNA level by S1 protection. RNAs were prepared from wild-type and *rne* strains grown at 32°C, or after a shift at 43°C for 10 min. *ftsA* and *ftsZ* probes SE1 and SE2 were labeled at their 5′ ends in the same reaction. T7pol.RNA lane: probe mixture annealed with T7 polymerase RNA made *in vitro* and digested with S1 nuclease.

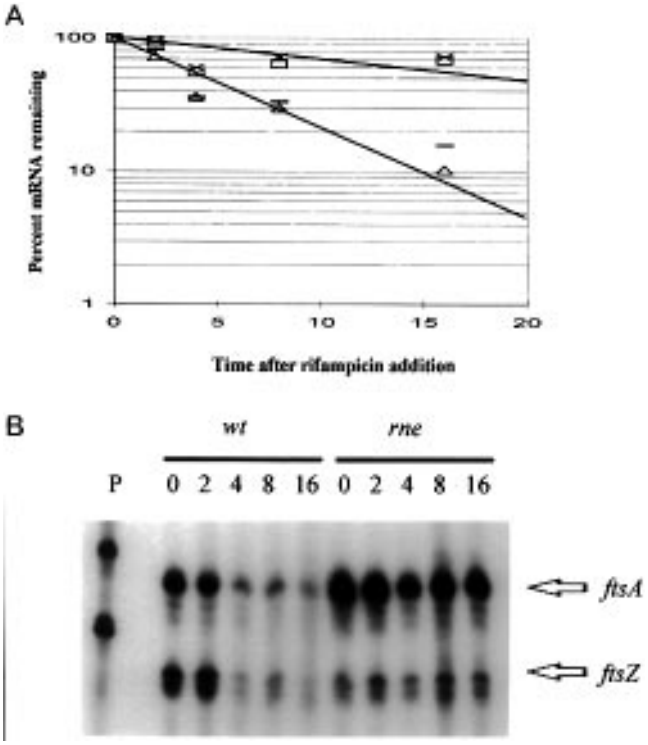

Figure 5. Measurement of *ftsA* and *ftsZ* mRNA stability at 43°C. Wild-type (*wt*) and mutant (*rne*) strains grown at 32°C were shifted to 43°C. After 10 min, rifampicin (150 µg/ml) was added and samples were taken for RNA extraction at 0, 2, 4, 8 and 16 min. The samples were analyzed by S1 protection. (**A**) The amount of protection products relative to the 0 min time sample is plotted as a function of the time after rifampicin addition. The values are the average of two experiments. Values for *ftsA* and *ftsZ* products in the *rne* background are symbolized by a cross and a rectangle respectively; in the wild-type background by a dash and a triangle respectively. (**B**) Raw data from one experiment is presented. Lane P contains the undigested probes mixture.

by S1 protection analysis in the rne^+ and *rne(ts)* strains (see Materials and Methods). Figure 4 shows that the ratio of *ftsA* mRNA to *ftsZ* mRNA increases in the *rne(ts)* strain at non-permissive temperature. This data had to be corrected for differential hybrid stability since a label ratio of 3.2 was obtained when the same probe mixture was hybridized with an *in vitro ftsA–ftsZ* mRNA synthesized from a T7 promoter (Fig. 4 and see Materials and Methods). After this normalization, the ratios of *ftsA* to *ftsZ* were 1.25 in the *rne* strain at non permissive temperature compared with 0.25 in wild-type background. At permissive temperature, these ratios were 0.4 versus 0.2 respectively. Therefore RNase E decreases the relative abundance of *ftsA* mRNA to *ftsZ* mRNA by a factor of ~5.

RNase E activity affects the stability of *ftsA* and *ftsZ* transcripts

The simplest explanation for the decrease of the *ftsA* to *ftsZ* ratio when RNase E is active is that cleavage at E1 and E3 sites makes *ftsA* mRNA preferentially susceptible to degradation by 3′→5′ exonucleases. To test this hypothesis, the chemical half-lives of *ftsA* and *ftsZ* 5′ regions were measured. As shown in Figure 5, the half-life for both mRNA species at 43°C was 4 min in rne^+ strain and >16 min in the RNase E-deficient strain. Thus RNase E cleavage equivalently affects the stability of both the upstream and downstream transcripts. Thus, the variation in the relative abundance of *ftsA* and *ftsZ* mRNA is not the mere consequence of their differential mRNA stability. Nevertheless, 10 min after the shift to 43°C, the amount of *ftsZ* mRNA in the *rne* strain was two to four times lower than in rne^+ strain (Figs 4 and 5), indicating that an event takes place between 0 and 10 min which leads to decrease the amount of *ftsZ* mRNA. In order to analyze this phenomenon further, the amount of *ftsA* and *ftsZ* mRNA were determined immediately after the shift to 43°C. Figure 6 shows the variations of the amounts of transcripts relative to those present at the time of the temperature shift. In the wild-type strain, the levels of *ftsA* and *ftsZ* mRNA increased after the temperature shift and reached a steady-state level three times higher than the previous one. A similar increase was observed in *rne(ts)* strain for *ftsA* mRNA. But, in contrast, no accumulation of *ftsZ* occurred in the *rne(ts)* strain shifted to 43°C. Since this difference is specific for the *rne(ts)* strain, we conclude that RNase E affects the mRNA *ftsA* to *ftsZ* ratio by another mechanism, independent from its effect on transcript stability. After the correction is made for hybrid differential stability these results indicate that in the *rne(ts)* background at 43°C, the absolute amounts of *ftsZ* and *ftsA* transcripts become nearly identical.

DISCUSSION

In many bacterial species, including *Haemophilus influenzae*, *Bacillus subtilis* and *E.coli*, the genes *ftsA* and *ftsZ* are contiguous within a cell division operon, with *ftsZ* just downstream of *ftsA*. A ratio of FtsZ to FtsA between 50 and 100 is necessary for correct cell division to occur in *E.coli* (15,16). Various mechanisms have been proposed to account for this protein ratio: greater transcription of *ftsZ* due to *ftsZ*-specific promoters (6,12) or more efficient translation of *ftsZ* versus *ftsA* (14). In this study, we report that a third mechanism also contributes to the different levels of expression of *ftsA* to *ftsZ*. We have identified two RNase E cleavage sites *in vivo* and *in vitro*, one in *ftsA* coding region, E1, and one in the *ftsA–ftsZ* intergenic region, E3. The site within *ftsA* coding

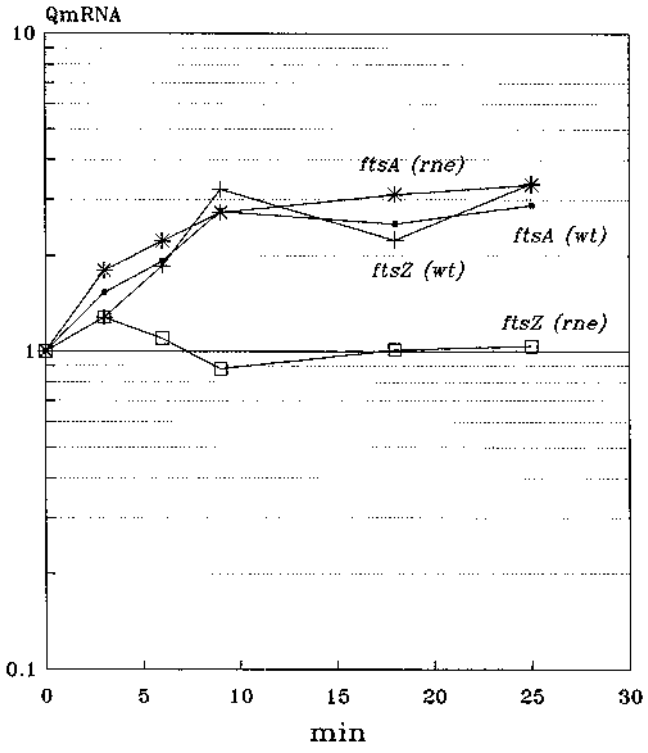

Figure 6. Accumulation of *ftsA* and *ftsZ* mRNA at 43°C. Wild-type (*wt*) and mutant (*rne*) strains grown at 32°C were shifted to 43°C, then samples were taken for RNA preparation at 0, 3, 6, 9, 18 and 25 min. The RNA samples were analyzed by S1 protection. The ordinate shows the ratio of the signal at different times to that at time zero for each given RNA species.

region is located at the position where a promoter, *ftsZ1p*, was previously thought to be present (6). Since *ftsZ1p* had been characterized solely on the basis of S1 mapping in an *rne*$^+$ context, no evidence now persists for its existence.

As a result of RNase E cleavage, *ftsA* RNA is destabilized in the cell. The current model of mRNA degradation (see ref. 28 for a review) is that endonucleases generate a free 3′ end which allows RNA to be attacked by 3′→5′ exonuclease(s). In some instances cleavages remove stem–loop structures which otherwise would have impeded exonuclease action, a situation which might apply to *ftsA* mRNA. Reports that RNase E is associated with polynucleotide phosphorylase (PNPase) suggests that PNPase might be responsible of the degradation of the RNA after the attack by RNase E (21,29). Although we have not addressed the question directly, it is likely that the destabilization of mRNA by RNase E cleavage also affects *ftsQ* mRNA.

We found that *ftsZ* mRNA is similarly destabilized when RNase E is active. This effect may be due to facilitated entry of the enzyme in the 5′ region of *ftsZ* mRNA (28), or to the presence of another cleavage site located downstream of the region studied. In any event, RNase E has a similar effect on the stability on both *ftsZ* and *ftsA* transcripts.

Despite this absence of differential effect, we found that in an RNase E-proficient strain, the *ftsA* to *ftsZ* mRNA ratio is approximately five times less than in a RNase E mutant at the non-permissive temperature, indicating that RNase E must somehow contribute to the expression ratio of the genes. The mechanism by which RNase E affects the transcript ratio appears to be complex and indirect. We observed that when an *rne*$^+$ strain is shifted to 43°C, the relative amount of *ftsA* and *ftsZ* transcripts increases within 20 min by a factor of approximately three (Fig. 6). This increase cannot be explained by a change in the copy number of the *ftsQAZ* plasmid used in our experiments since pBR322 derivatives are insensitive to a temperature shift from 35 to 43°C (30). Our preliminary results indicate that some promoters contributing to *ftsAZ* expression are involved. When an *rne*(ts) strain is shifted to the non-permissive temperature, the amount of *ftsA* mRNA (relative to total RNA) increases approximately three times within 20 min (Fig. 6). Such an increase can be entirely accounted for by a change of *ftsA* mRNA half-life from 4 to >16 min, suggesting that no transcriptional activation of *ftsA* occurs in the RNase E-defective context. The situation is different for *ftsZ* transcripts, whose level does not increase despite greater stability, suggesting decreased transcription. This decrease does not result from reduced transcription from promoters *ftsZ2p*, *ftsZ3p* or *ftsZ4p*, located within *ftsA*, since primer extension experiments have indicated that the activity of these promoters is unaffected when RNase E is inactivated (data not shown). The same experiments suggest that transcripts initiating from these promoters are not exceptionally unstable. Yet our results indicate that the relative level of *ftsA/ftsZ* 5′ region transcripts become close to 1 in the *rne* mutant at 43°C (Fig. 6, corrected for probe efficiency). Therefore our current hypothesis is that lack of RNase E processing creates a situation, that brings about premature transcriptional termination before transcription from *ftsZ2p*, *ftsZ3p* or *ftsZ4p* reaches *ftsZ*.

Our results indicating that the ratio of *ftsA* to *ftsZ* mRNA in a wild-type strain grown at 32°C is ~0.25 concern exclusively selected segments located at the 5′ ends of the genes, and cannot be easily extrapolated to functional transcripts. The protein ratio is determined by the ratio of the full-length *ftsA* transcripts to the full-length *ftsZ* transcripts ratio and this ratio may be much more than 0.25.

There is no direct evidence that the cleavages at E1 and E3 or other RNase E-dependent processes affecting *ftsA* or *ftsZ* expression are important for the control of cell division. However Goldblum and Apirion (17) reported that upon shifting an *rne(ts)* mutant to the non-permissive temperature, cell division stops immediately whereas mass increase slows down but does not halt for 3 h. The arrest of cell division might be an indirect consequence of the mutation, or alternatively it might be a direct effect of altering the ratio of *ftsZ* to *ftsA* expression.

ACKNOWLEDGEMENTS

We are grateful to A. Carpousis for providing purified RNase E enzyme, advice on experimental conditions and for suggesting the premature termination hypothesis, and to D. Lane and P. Casaz for helpful discussions on the manuscript. This work was supported in part by the Université Paul Sabatier and by contract no. 6269 from the Association pour la Recherche sur le Cancer.

REFERENCES

1 Lutkenhaus, J. (1993) *Mol. Microbiol.*, **9**, 403–409.
2 Ayala, J.A., Garrido, T., de Pedro, M.A. and Vicente, M. (1994) In Ghuysen, J.-M. and Hakenbecck, R. (eds) *Bacterial Cell Wall.* Elsevier Science *B.V,* pp. 73–101.
3 Ward, J.E. and Lutkenhaus, J. (1985) *Cell,* **42**, 941–949.
4 Dai, K. and Lutkenhaus J. (1991) *J. Bacteriol.*, **173**, 3500–3506.

5 Tétart, F., Albigot, R., Conter, A., Mulder, E. and Bouché, J.-P. (1992) *Mol. Microbiol.*, **6**, 621–627.
6 Aldea, M., Garrido, T., Pla, J. and Vicente, M. (1990) *EMBO J.*, **9**, 3787–3794.
7 Tétart, F. and Bouché, J.-P. (1992) *Mol. Microbiol.*, **6**, 615–620.
8 Carson, M.J., Barondess, J. and Beckwith, J. (1991) *J. Bacteriol.*, **173**, 2187–2195.
9 Wang, H. and Gayda, R.C. (1992) *Mol. Microbiol.*, **6**, 2517–2524.
10 Pla, J., Sanchez, M., Palacios, P., Vicente, M. and Aldea, M. (1991) *Mol. Microbiol.*, **5**, 1681–1686.
11 Bi, E. and Lutkenhaus, J. (1991) *Nature*, **354**, 161–164.
12 Yi, Q.-M., Rockenbach, S., Ward, J.E. and Lutkenhaus, J. (1985) *J. Mol. Biol.*, **184**, 399–412.
13 Garrido, T., Sanchez, M., Palacios, P., Aldea, M. and Vicente, M. (1993) *EMBO J.*, **12**, 3957–3965.
14 Mukherjee, A. and Donachie, W.D. (1990) *J. Bacteriol.*, **172**, 6106–6111.
15 Dai, K. and Lutkenhaus, J. (1992) *J. Bacteriol.*, **174**, 6145–6151.
16 Dewar, S.J., Begg, K.J. and Donachie, W.D. (1992) *J. Bacteriol.*, **174**, 6314–6316.
17 Goldblum, K. and Apirion, D. (1981) *J. Bacteriol.*, **146**, 128–132.
18 Sarmientos, P., Sylvester, J.E., Contente, S. and Cashel, M. (1983) *Cell*, **32**, 1337–1346.
19 Cam, K., Oberto, J. and Weisberg, R.A. (1991) *J. Bacteriol.*, **173**, 734–740.
20 Theisen, P.W., Grimwade, J.E., Leonard, A.C., Bogan, J.A. and Helmstetter, C.E. (1993) *Mol. Microbiol.*, **10**, 575–584.
21 Carpousis, A.J., Van Houwe, G., Ehretsmann, C. and Krisch, H.M. (1994) *Cell*, **76**, 889–900.
22 Ehretsmann, C., Carpousis, A.J. and Krisch, H.M. (1992) *Genes Dev.*, **6**, 149–159.
23 McDowall, K.J., Lin-Chao, S. and Cohen, S.N. (1994) *J. Biol. Chem.*, **269**, 10790–10796.
24 McDowell, K.J., Kaberdin, V.R., Wu, S.W., Cohen, S.N. and Lin-Chao, S. (1995) *Nature*, **374**, 287–290.
25 Loayza, D., Carpoussis, A.J. and Krisch, H.M. (1991) *Mol. Microbiol.*, **5**, 715–725.
26 Alifano, P., Rivellini, F., Piscitelli, C., Arraiano, C.M., Bruni, C.B. and Carlomagno, M.S. (1994) *Genes Dev.*, **8**, 3021–3031.
27 Yarchuk, O., Jacques, N., Guillerez, J. and Dreyfus, M. (1992) *J. Mol. Biol.*, **226**, 581–596.
28 Higgins, C.F., Causton, H.C., Dance, G.S.C. and Mudd, H.A. (1993) In Belasco, J. and Brawerman, G. (eds) *Control of Messenger RNA Stability.* Academic Press, San Diego, pp. 13–30.
29 Py, B., Causton, H., Mudd, E.A. and Higgins, C.F. (1994) *Mol. Microbiol.*, **14**, 717–729.
30 Lin-Chao, S. and Cohen, S.N. (1991) *Cell*, **65**, 1233–1242.